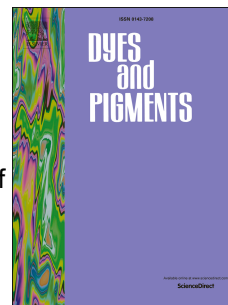


Accepted Manuscript

Fluorescence sensing of Ag^+ ions by desulfurization of an acetylthiourea derivative of 2-(2-hydroxyphenyl)benzothiazole

Keum Saem Hwang, Ka Young Park, Da Bin Kim, Suk-Kyu Chang



PII: S0143-7208(17)31424-9

DOI: [10.1016/j.dyepig.2017.08.041](https://doi.org/10.1016/j.dyepig.2017.08.041)

Reference: DYPI 6203

To appear in: *Dyes and Pigments*

Received Date: 29 June 2017

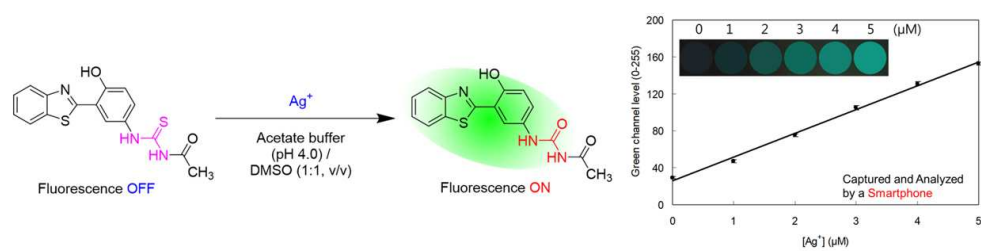
Revised Date: 23 August 2017

Accepted Date: 23 August 2017

Please cite this article as: Hwang KS, Park KY, Kim DB, Chang S-K, Fluorescence sensing of Ag^+ ions by desulfurization of an acetylthiourea derivative of 2-(2-hydroxyphenyl)benzothiazole, *Dyes and Pigments* (2017), doi: 10.1016/j.dyepig.2017.08.041.

This is a PDF file of an unedited manuscript that has been accepted for publication. As a service to our customers we are providing this early version of the manuscript. The manuscript will undergo copyediting, typesetting, and review of the resulting proof before it is published in its final form. Please note that during the production process errors may be discovered which could affect the content, and all legal disclaimers that apply to the journal pertain.

Graphical Abstract



Fluorescence sensing of Ag^+ ions by desulfurization of an acetylthiourea derivative of 2-(2-hydroxyphenyl)benzothiazole

Keum Saem Hwang, Ka Young Park, Da Bin Kim, and Suk-Kyu Chang*

Department of Chemistry, Chung-Ang University, Seoul 06974, Republic of Korea

*Corresponding author. Tel.: +82 2 820 5199; Fax: +82 2 825 4736.

E-mail address: skchang@cau.ac.kr (S.-K. Chang)

Abstract:

A novel Ag^+ -selective reaction-based probe based on an acetylthiourea derivative of 2-(2-hydroxyphenyl)benzothiazole dye was investigated. The designed probe showed pronounced off-on type fluorescence signaling behavior in the presence of Ag^+ ions via Ag^+ -induced desulfurization of acetylthiourea to acetylurea. The signaling was superior to the analogous thioamide-to-amide conversion in terms of both speed and signaling contrast. Interference from thiophilic Hg^{2+} ions was effectively suppressed using the chelating agent EDTA as a masking agent. The practical application of the system to the detection of Ag^+ in simulated wastewater with a detection limit of 0.76 μM using a smartphone as an easy-to-use data capturing and processing device was successfully demonstrated.

Keywords: Ag^+ sensing; Fluorescence; Desulfurization; Acetylthiourea; 2-(2-hydroxyphenyl)benzothiazole; Smartphone.

1. Introduction

Silver and silver-containing compounds are important resources that are used in the electronics, photographic, imaging, and pharmaceutical industries [1–4]. Ag^+ exhibits rich biological chemistry, and acts as a widely used antibacterial agent [5] and a transcriptional initiator in plants [6] and mammals [7,8]. However, when the concentration of Ag^+ ions becomes sufficiently high, silver-related technologies can lead to potentially hazardous side effects in the environment [9–12]. It is known that silver ions can deactivate sulfhydryl enzymes and are also capable of combining with the imidazole, amine, and carboxyl groups of various metabolites, which can lead to harmful effects in human beings [3,4,13]. Repeated exposure to Ag^+ can produce anemia, cardiac enlargement, growth retardation, and degenerative changes in animals [14]. The United States Environmental Protection Agency (USEPA) recommends a maximum concentration of silver ions in drinking water of 100 $\mu\text{g/L}$ [15]. Therefore, the development of rapid, selective, and sensitive methods of detecting Ag^+ ions is essential for both environmental protection and human health [16].

Hitherto, various instrumental techniques such as atomic absorption spectrometry, inductively coupled plasma mass spectrometry, and electrochemical methods have been used to detect silver ions; however, all of these require expensive instruments and/or time-consuming procedures [17–23]. Optical methods such as colorimetry and fluorescence spectroscopy are more convenient than these traditional techniques due to their high sensitivities, noninvasive natures, and suitability for real-time detection [24,25].

A number of elaborately designed optical sensors and probes have been developed for the determination or visualization of chemically, biologically, and environmentally important chemical species [24,26,27]. Recently, reaction-based probes have attracted much research interest because they provide a number of advantages that enable the design of selective and efficient signaling systems for the detection of various important metal ions, anions, and oxidants [28]. Especially, fluorescence probes that utilize reaction-based transformations for the detection of intrinsically quenching ions of Hg^{2+} , Cu^{2+} , and Ag^+ are particularly attractive because they afford off-on type signaling responses, which are more desirable than on-off type sensing systems.

Desulfurization reactions have been one of the most successful strategies of the many sophisticated approaches to the design of reaction-based probes for thiophilic metal ions such as Hg^{2+} , Cu^{2+} , and Ag^+ . Czarnik and co-workers reported the first fluorescent Hg^{2+} -selective probe based on the sulfur to oxygen exchange reaction of anthracene-thioamide, which is promoted by Hg^{2+} and Ag^+ ions [29]. After this, a number of probes using desulfurization processes have been developed for the thiophilic metal ions. However, when compared with probes for Hg^{2+} and Cu^{2+} ions, Ag^+ -selective probes have been less widely investigated. Representative examples of reaction-based probes for the determination of Ag^+ ions are developed using desulfurization of the thioamide group of 9-[(methylamino)thiocarbonyl]anthracene [29] and the deprotection of 1,3-dithiane-modified BODIPY [30]. Desulfurization of a coumarin derivative containing an *N'*-acetylthiourea group [31], deselenation of rhodamine B selenolactone [32], and irreversible tandem ring-opening and formation of oxazoline from rhodamine spirolactam are also noteworthy [33].

In reality, many Ag^+ -selective sensors and probes frequently suffered from significant interference from other commonly encountered transition metal ions, such as Hg^{2+} and Cu^{2+} [34]. A valuable tactic for circumventing this interference is the use of a chelating agent that can discriminate between the target and the interfering ions. In the design of Ag^+ -selective sensors, EDTA and thiosulfate have been successfully used to mask responses from Hg^{2+} and Cu^{2+} ions [35]. However, we could not find any literature on using such chelating agents for the realization of Ag^+ -selective reaction-based probes.

In this paper, a new Ag^+ -selective fluorescence signaling probe based on the Ag^+ -induced desulfurization of an acetylthiourea derivative of 2-(2-hydroxyphenyl)benzothiazole dye is described. The designed probe employs the acetylthiourea group as a switch to turn-on the Ag^+ -induced fluorescence revival of 2-(2-hydroxyphenyl)benzothiazole. 2-(2-Hydroxyphenyl)benzazoles are versatile fluorescent compounds that exhibit unique excited-state intramolecular proton transfer (ESIPT) phenomena [36]. Moreover, the 4-substituted amine analogue 2-(5-amino-2-hydroxyphenyl)benzothiazole and its benzoxazole analogue have been utilized as platforms for the design of ESIPT-type signaling probes for a number of important species. These are based on the generation of an ESIPT-capable fluorophore by deprotection of O-protected functional groups on the phenol moiety, such as deallylation for detection of Pd^{2+} [37], vinyl ether hydrolysis for detection of Hg^{2+} [38], desilylation for detection of fluoride [39,40], and phenylboronate hydrolysis for detection of H_2O_2 [41]. The present investigation shows that an acetylthiourea-based probe exhibited selective signaling behavior towards thiophilic Ag^+ ions via a smooth desulfurization process. Using EDTA as a masking agent for

interfering Hg^{2+} ions, we could realize an exclusive Ag^+ -selective signaling probe system. To demonstrate a practical application of the system, the determination of Ag^+ in simulated wastewater using a readily available smartphone was conducted.

2. Experimental

General: 5-Aminosalicylic acid, 2-aminothiophenol, 2,4-bis(4-methoxyphenyl)-2,4-dithioxo-1,3,2,4-dithiadiphosphetane (Lawesson's reagent), acetyl chloride, potassium thiocyanate, and all spectroscopic grade solvents were purchased from Aldrich Chemical Co. Polyphosphoric acid was obtained from Alfa Aesar. Column chromatography was performed using silica gel (240 mesh). ^1H NMR (300 MHz) and ^{13}C NMR (150 MHz) spectra were measured using Varian Gemini 2000 and Varian VNS spectrometers, and were referenced to the residual solvent signals. UV-vis spectra were recorded using a Scinco S-3100 spectrophotometer. Fluorescence spectra were measured using a Scinco FS-2 fluorescence spectrophotometer. High resolution mass spectra (HRMS) using fast atom bombardment (FAB) and electrospray ionization (ESI) were recorded on JEOL JMS-700 and Bruker Compact mass spectrometer, respectively. FT-IR measurements were carried out using a Thermo Scientific Nicolet 6700 spectrophotometer using KBr pellets.

Preparation of probe 2. A mixture of acetyl chloride (887 mg, 11.3 mmol) and potassium thiocyanate (2.19 g, 22.5 mmol) in acetonitrile (25 mL) was stirred under reflux for 1 h. After the solution was cooled to room temperature, 2-(5-amino-2-hydroxyphenyl)benzothiazole **1** (500 mg, 2.06 mmol) was added, and the reaction mixture was stirred at room temperature for 1.5 h. The resulting precipitate was

filtered, washed with acetonitrile several times, and dried to obtain 608 mg (86%) of probe **2** as a grey powder. mp: 240 °C (decomposed). ^1H NMR (300 MHz, DMSO- d_6): δ 12.36 (s, 1H), 11.73 (s, 1H), 11.49 (s, 1H), 8.42 (d, $J = 2.7$ Hz, 1H), 8.15 (d, $J = 7.8$ Hz, 1H), 8.06 (d, $J = 8.0$ Hz, 1H), 7.56–7.54 (m, 2H), 7.45 (t, $J = 7.5$ Hz, 1H) 7.15 (d, $J = 8.7$ Hz, 1H), 2.17 (s, 3H); ^{13}C NMR (150 MHz, DMSO- d_6) δ 179.4, 172.8, 163.9, 154.6, 151.5, 134.8, 130.0, 129.2, 126.6, 125.2, 124.5, 122.3, 122.1, 118.6, 117.1, 24.0. IR (KBr): $\nu_{\text{max}}/\text{cm}^{-1}$ 3425 (br, O–H stretch), 3220 (m, N–H stretch), 3149 (m, N–H stretch), 3060 (w, Ar C–H stretch), 1702 (s, C=O stretch), 1547 (m, N–H bend), 1538 (m, N–H bend), 1547 (s, C=S stretch). HRMS: (ESI+); calcd for $[\mathbf{2}+\text{Na}]^+$ ($\text{C}_{16}\text{H}_{13}\text{N}_3\text{NaO}_2\text{S}_2$), $m/z = 366.0341$, observed: 366.0341.

Preparation of probe 4. Acetamide derivative **3** was prepared by the reaction of **1** with acetyl chloride following a literature method [42]. Thioamide **4** was prepared by the reaction of acetamide **3** with Lawesson's reagent. A mixture of acetamide **3** (284 mg, 1.0 mmol) and Lawesson's reagent (459 mg, 1.1 mmol) in toluene (20 mL) was refluxed for 18 h. The resulting reaction mixture was cooled, evaporated, and partitioned between dichloromethane and water. The organic phase was separated and evaporated to obtain probe **4** as a brown powder. Purification was carried out by column chromatography (CH_2Cl_2 :MeOH, 20:1 v/v). Yield: 52%. mp: 250 °C (decomposed). ^1H NMR (300 MHz, DMSO- d_6): δ 11.63 (s, 2H), 8.63 (d, $J = 2.6$ Hz, 1H), 8.21–8.12 (m, 1H), 8.06 (d, $J = 8.0$ Hz, 1H), 7.86 (dd, $J = 8.8, 2.7$ Hz, 1H), 7.63–7.51 (m, 1H), 7.50–7.40 (m, 1H), 7.10 (d, $J = 8.8$ Hz, 1H), 2.62 (s, 2H); ^{13}C NMR (150 MHz, DMSO- d_6) δ 198.7, 164.2, 154.0, 151.4, 134.5, 131.9, 127.7, 126.5, 125.1, 123.1, 122.2, 122.1, 118.1, 116.7, 34.8. IR (KBr): $\nu_{\text{max}}/\text{cm}^{-1}$ 3450 (br w, O–H

stretch), 3164 (m, N–H stretch), 3060 (w, Ar C–H stretch), 2991 (w, Ar C–H stretch), 2939 (w, Ar C–H stretch), 1548 (m, N–H bend), 1498 (m, C–N stretch), 1153 (s, C=S stretch). HRMS: (FAB+); calcd for [4]⁺ (C₁₅H₁₃N₂OS₂), $m/z = 301.0400$, observed: 301.0407.

Preparation of stock solutions. Stock solutions of **2** and **4** (5.0×10^{-4} M) were prepared in spectroscopic grade DMSO. Stock solutions (1.0×10^{-2} M) of metal ions were prepared in deionized water or simulated wastewater. Simulated wastewater was prepared in deionized water following the literature [43,44].

Measurement of signaling behavior. The fluorescence signaling behaviors of probes **2** and **4** toward Ag⁺ were measured in mixed solutions of acetate buffer (pH 4.0) and DMSO (1:1, v/v). Solutions were prepared for measurement by adding the probe stock solution (30 μ L, 5.0×10^{-4} M), acetate buffer (150 μ L, 2.0×10^{-1} M), EDTA (15 μ L, 1.0×10^{-1} M), and metal ion stock solutions (15 μ L, 1.0×10^{-2} M) to a 10 mL vial. The solutions were diluted with distilled water and DMSO to give a final volume of 3.0 mL (buffer solution : DMSO = 1:1, v/v for **2** and 1:9, v/v for **4**). The final concentrations of the probe, acetate buffer, EDTA, and metal ions in the measuring solutions were 5.0×10^{-6} M, 1.0×10^{-2} M, 5.0×10^{-4} M, and 5.0×10^{-5} M, respectively.

Detection limit of Ag⁺ ions. Following IUPAC recommendation, the detection limit of Ag⁺ was assessed by the equation $3s_{bl}/m$, where s_{bl} is the standard deviation of the

blank measurements (number of measurements = 15) and m is the calibration sensitivity obtained from the slope of the calibration plot.

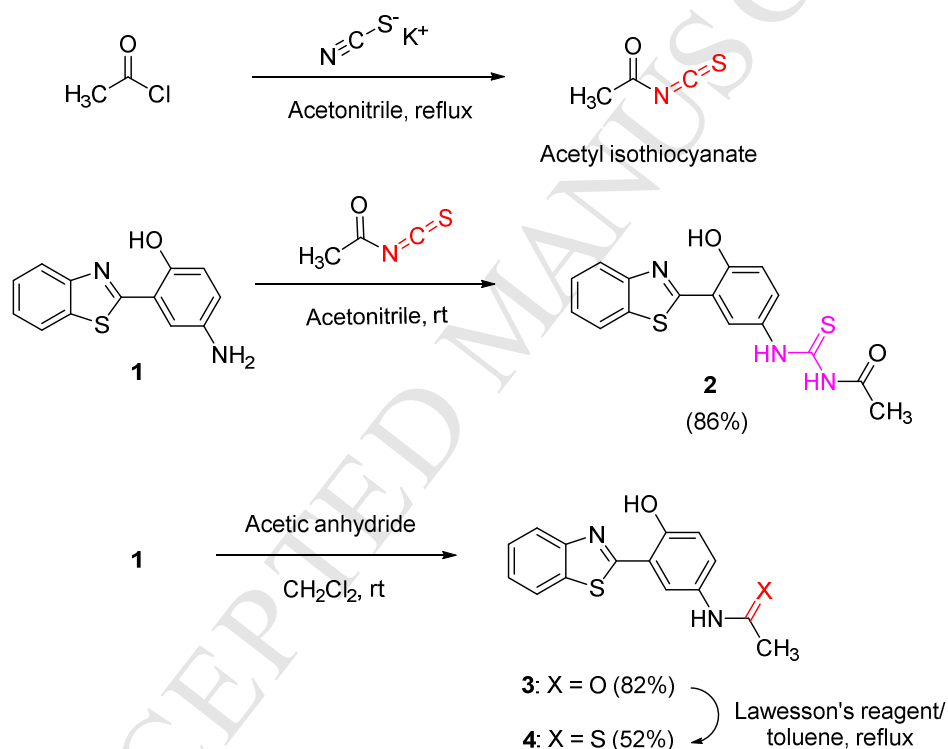
Smartphone-assisted detection of Ag^+ ions in simulated wastewater. Images of the signaling solutions prepared from standard solutions with varying Ag^+ concentrations were captured using a smartphone in a dark room and used to plot the corresponding calibration curve. Calculated amounts of simulated wastewater stock solutions containing Ag^+ , acetate buffer, EDTA, and probe **2** were sequentially added to a vial, and the resulting solutions were diluted to 3.0 mL using simulated wastewater and DMSO. The final concentrations of **2**, EDTA, and Ag^+ in the test solutions were 5.0×10^{-6} M, 5.0×10^{-4} M, and $0\text{--}5.0 \times 10^{-6}$ M, respectively, in a mixture of acetate buffered (pH 4.0, final concentration = 1.0×10^{-2} M) simulated wastewater and DMSO (1:1, v/v). Images of the solutions under a UV light (365 nm) were obtained in a dark room using a smartphone (Samsung Electronics Co., Ltd., Galaxy S7). The green channel levels of the resulting images were estimated using a smartphone-embedded RGB Grabber application. Using a plot of this value vs. $[\text{Ag}^+]$ as a working calibration curve, the concentration of Ag^+ in simulated wastewater was estimated.

3. Results and discussion

The designed acetylthiourea-based probe **2** was prepared by the reaction of benzothiazolyl-aminophenol **1** with acetyl isothiocyanate, as outlined in Scheme 1. Benzothiazolyl-aminophenol **1** was prepared by the reaction of 2-aminothiophenol with 5-aminosalicylic acid in polyphosphoric acid following a reported procedure (79% yield)

[37]. The reaction of **1** with acetyl isothiocyanate, which was prepared by the treatment of potassium thiocyanate with acetyl chloride, in acetonitrile afforded desired acetylthiourea **2** in a good yield (86%). Thioamide **4** was prepared as a control compound by the thionation of acetamide **3**, which was obtained by the reaction of **1** with acetyl chloride (DMF, 91% yield), with Lawesson's reagent (toluene, 52% yield).

Scheme 1. Preparation of Ag⁺-selective acetylthiourea (**2**) and thioamide (**4**) probes.



The signaling behaviors of probes **2** and **4** towards common metal ions were investigated by UV-vis and fluorescence spectroscopy. Acetylthiourea **2** showed weak emission at 415 nm and broad emission at 490 nm in an acetate buffer (pH 4.0) solution containing 50% DMSO. Upon treatment with metal ions, prominent fluorescence responses to Hg²⁺ and Ag⁺ ions were observed (Figure S1, Supplementary data). That is

due to the metal-induced desulfurization of acetylthiourea **2** to produce acetylurea **5** (vide infra). In contrast to this, no considerable changes in the UV–vis spectrum of **2** were observed on exposure to the surveyed metal ions (Figure S2, Supplementary data).

For most analytical purposes, selectivity for a single target metal ion is far more desirable than multiple responses from closely related metal ions. We attempted to improve the metal ion selectivity of **2** by fine-tuning the signaling conditions by altering the solvent composition and pH, as well as the use of extra masking agents that could interact differently with Hg^{2+} and Ag^+ ions. After a systematic survey, we found that pronounced peak selectivity for Ag^+ ions could be realized by using EDTA as a masking agent. Interference from Hg^{2+} ions was effectively suppressed by complex formation, allowing exclusive selectivity of **2** towards Ag^+ ions to be obtained. For instance, in an acetate-buffered solution containing EDTA (10 equiv) and DMSO (1:1, v/v), probe **2** showed marked fluorescence enhancement only with Ag^+ ions (Figure 1 and Figure S3, Supplementary data). The color of the solution under illumination with a UV lamp ($\lambda_{\text{ex}} = 365 \text{ nm}$) changed from a faint dark blue to a bright greenish blue on exposure to Ag^+ , and the fluorescence intensity enhancement of **2** at 490 nm (I/I_0) was 53-fold. Other metal ions showed negligible responses ($I/I_0 = 0.83\text{--}1.32$).

It is worth noting that we initially aimed to develop the analogous thioamide **4** as an Ag^+ -selective probe. However, thioamide **4** showed less pronounced Ag^+ -selectivity (Figure S4, Supplementary data) as well as much slower signaling behavior than acetylthiourea **2** (Figure S5, Supplementary data). The large increase in signaling speed of **2** as compared with thioamide **4** is due to the formation of intramolecular hydrogen bonding between the acetylthiourea moiety, and is in good agreement with the results obtained by Tsukamoto et al., for a 7-hydroxycoumarin-based acetylthiourea compound

[30].

The highly Ag^+ -selective signaling of **2** in the present system can be rationalized by referring to the formation constants ($\log K_f$) of the EDTA complexes of Ag^+ and Hg^{2+} , which are 7.32 and 21.7, respectively [45]. However, below pH 10.24, EDTA (H_4Y) does not fully dissociate into its complex formation form, Y^{4-} , and therefore the conditional formation constant ($K_f' = \alpha_{Y^{4-}} K_f$) should be considered, where $\alpha_{Y^{4-}}$ denotes the fraction of EDTA in its fully deprotonated form (Y^{4-}). At pH 4.0, $\alpha_{Y^{4-}}$ for EDTA is 3.8×10^{-9} [45]. Therefore, the conditional formation constants ($\log K_f'$) of Ag^+ and Hg^{2+} at pH 4.0 are -1.10 and 13.3, respectively. The value of the Ag^+ -EDTA complex at pH 4.0 ($\log K_f' = -1.10$) enables us to postulate that the Ag^+ ions weakly interact with EDTA, thereby a reaction between Ag^+ and acetylthiourea should be possible. On the other hand, Hg^{2+} is tightly complexed to EDTA at pH 4 ($\log K_f' = 13.3$), and so cannot participate in the desulfurization signaling process. Meanwhile, the selective sensing of Ag^+ ions using probe **2** in the presence of competing Hg^{2+} ions is believed to be infeasible under physiological conditions, because the conditional formation constants ($\log K_f'$) of both Ag^+ and Hg^{2+} ions at physiologically relevant pH 7.4 are high (4.33 and 18.7, respectively).

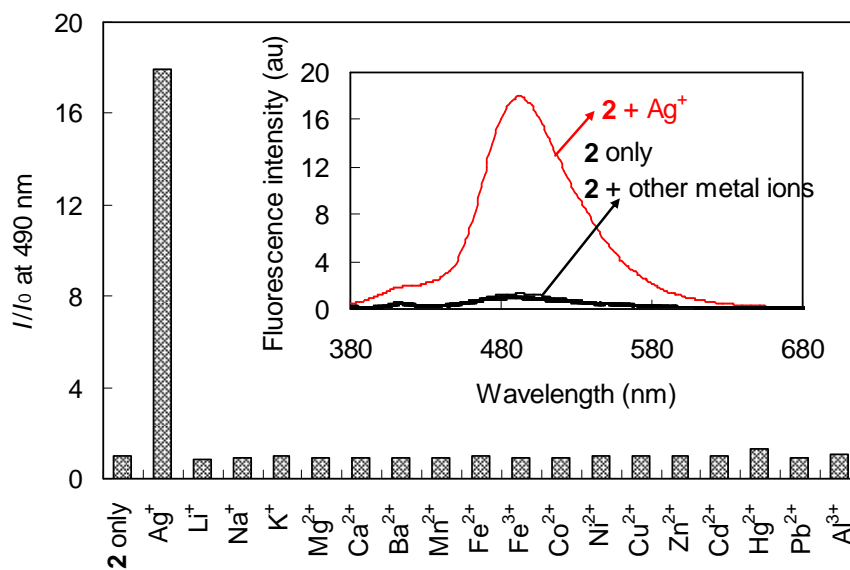


Figure 1. Ag^+ -selective signaling of **2** in the presence of a masking agent (EDTA). Inset: changes in fluorescence spectrum. $[\mathbf{2}] = 5.0 \times 10^{-6}$ M, $[\text{M}^{n+}] = 5.0 \times 10^{-5}$ M, and $[\text{EDTA}] = 5.0 \times 10^{-4}$ M in a mixture of an acetate buffer (pH 4.0, final concentration = 10 mM) and DMSO (1:1, v/v). $\lambda_{\text{ex}} = 366$ nm.

Sensing of Ag^+ is ascribable to the conversion of acetylthiourea **2** to acetylurea **5** (Scheme 2). The fluorescence of the 2-(2-hydroxyphenyl)benzothiazole framework, which is suppressed in acetylthiourea due to the presence of the thiocarbonyl group, is recovered after the conversion to acetylurea. The postulated conversion was confirmed by ^1H NMR and mass spectroscopy. Upon treatment of **2** with Ag^+ ions, the ^1H NMR spectrum changed to that of acetylurea **5** (Figure 2). Particularly, the resonance of acetylthiourea NH protons at 11.49 and 12.36 ppm were converted to acetylurea NH protons at 10.46 and 10.65 ppm, respectively. In addition, in the mass measurement, an intense molecular ion peak for **5** was observed at $m/z = 350.0571$ (calcd for $\text{C}_{16}\text{H}_{13}\text{N}_3\text{NaO}_3\text{S} = 350.0570$) after conversion (Figure S6, Supplementary data).

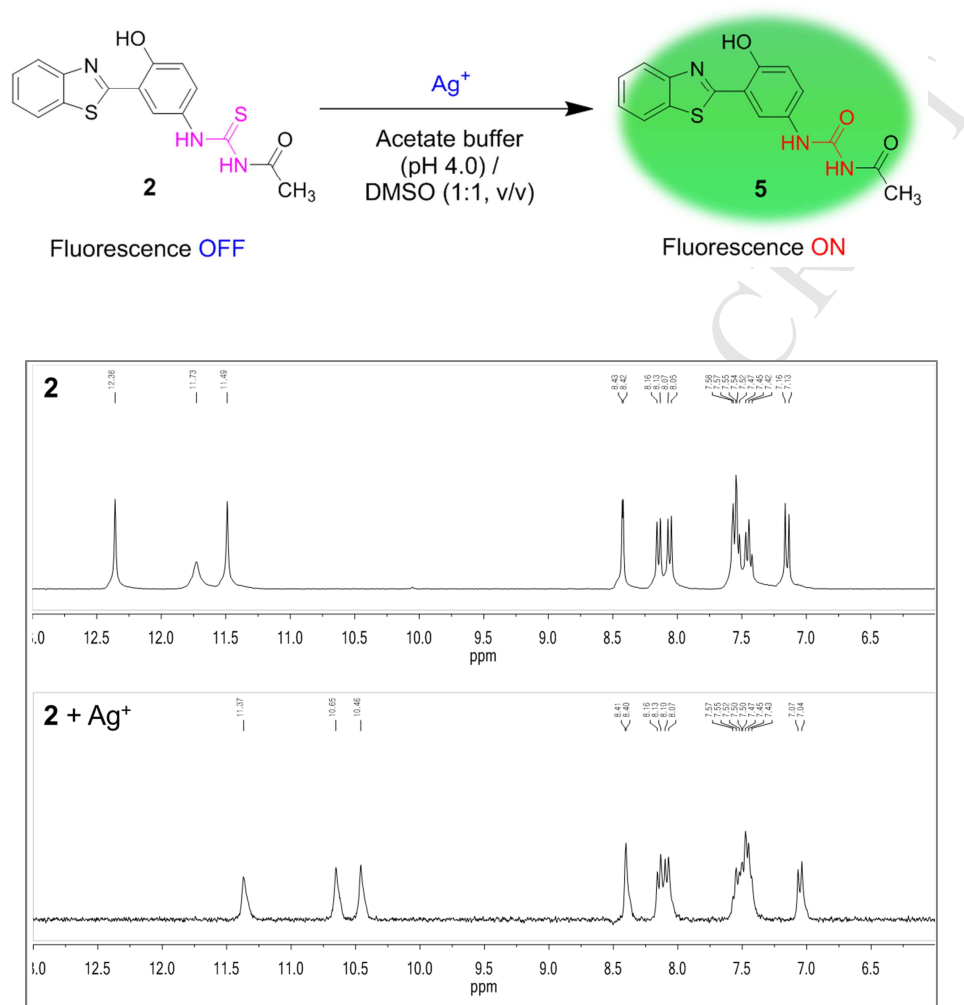
Scheme 2. Ag⁺ signaling by desulfurization of **2**.

Figure 2. Partial ¹H NMR spectra of **2** and **2** in the presence of Ag⁺ (**2 + Ag⁺**). [**2**] = 5.0 × 10⁻³ M and [AgClO₄] = 1.0 × 10⁻² M in DMSO-*d*₆. The spectrum of (**2 + Ag⁺**) was obtained after purification of the signaling product by passing it through a silica plug.

Competitive detection of a specific target analyte over other commonly coexisting species is important for practical applications of probes. The Ag⁺-selective signaling of probe **2** was not significantly affected by a background of other common metal ions (Figure 3). The interference as expressed by the change in fluorescence intensity ratio at

490 nm ($I_{(\text{Metal ion}+\text{Ag(I)})}/I_{\text{Ag(I)}}$) varied narrowly between 0.96 for Li^+ and 1.02 for Zn^{2+} ions. This observation indicates that probe **2** could be used for the selective detection of Ag^+ in analytes that are commonly encountered in chemical and environmental sciences.

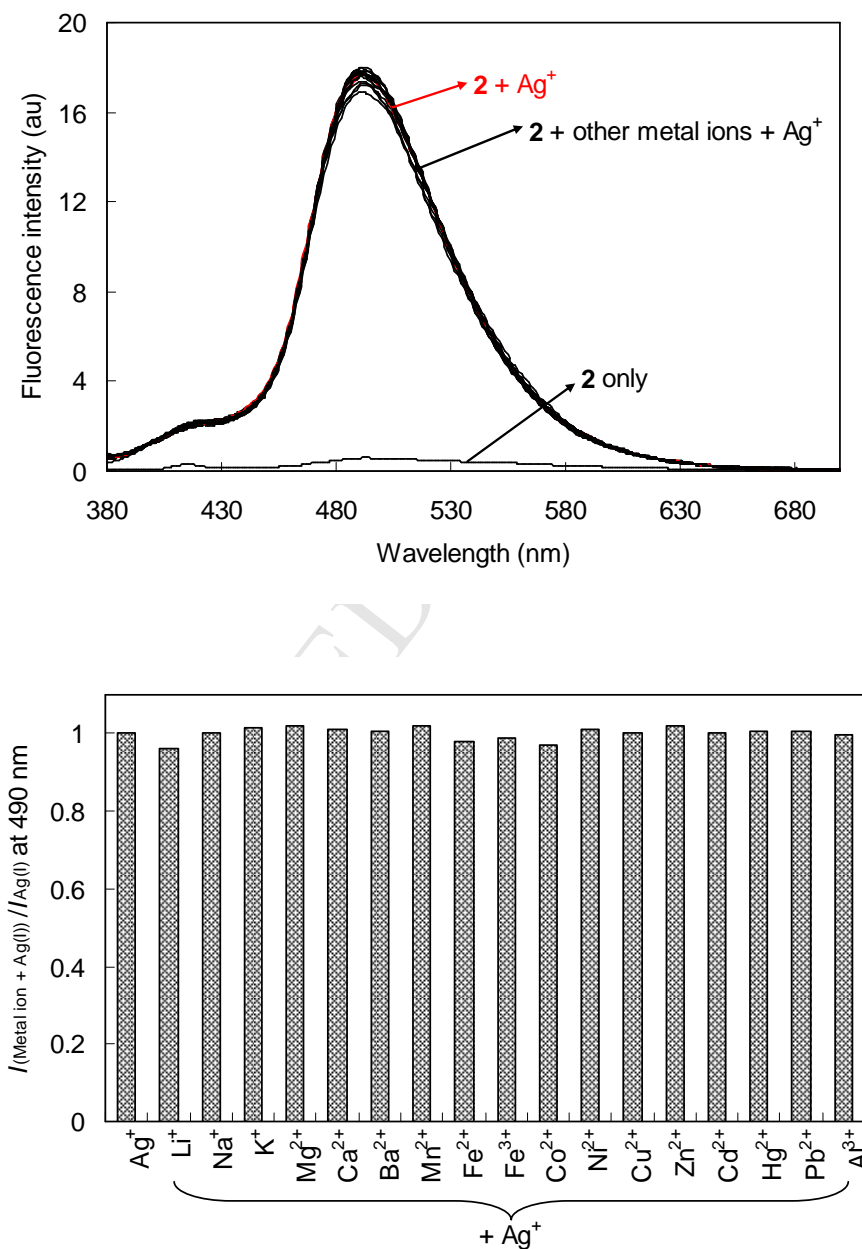


Figure 3. Changes in fluorescence spectrum of **2** when detecting Ag^+ in the presence of

various metal ions as background (upper). Fluorescence intensity ratio ($I_{(\text{Metal ion}+\text{Ag(I)})}/I_{\text{Ag(I)}}$) of **2** at 490 nm (lower). $[\text{Ag}^+] = [\text{M}^{\text{n}+}] = 5.0 \times 10^{-5}$ M. Other conditions are the same as those in Figure 1.

The pH-dependent signaling profile of probe **2** shows that most pronounced signaling contrast between the two pertinent metal ions (Ag^+ and Hg^{2+}), as expressed by the fluorescence intensity ratio ($I_{\text{Ag(I)}}/I_{\text{Hg(II)}}$) at 490 nm, was observed at pH 4.0 (Figure 4).

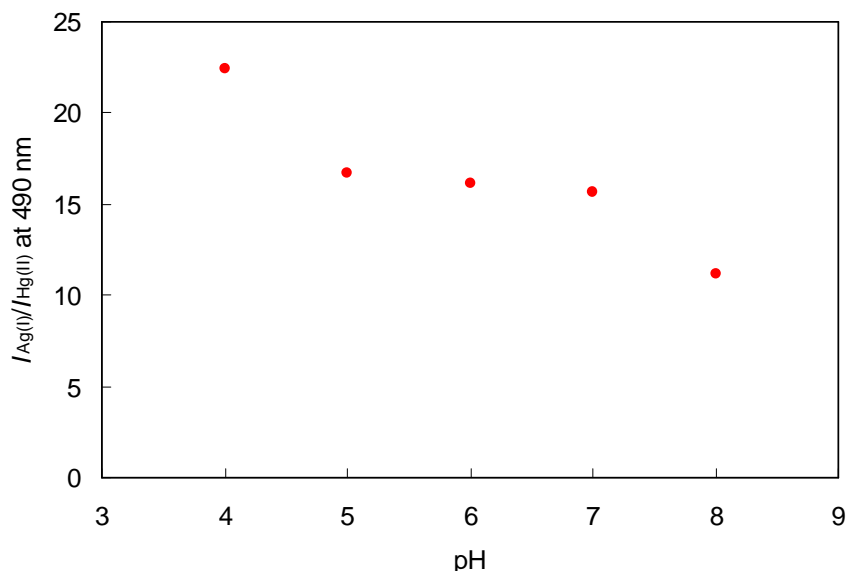


Figure 4. Effect of pH on the selective fluorescence signaling of Ag^+ by **2** as expressed by the fluorescence intensity ratio $I_{\text{Ag(I)}}/I_{\text{Hg(II)}}$ at 490 nm. $[\mathbf{2}] = 5.0 \times 10^{-6}$ M, $[\text{Ag}^+] = [\text{Hg}^{2+}] = 5.0 \times 10^{-5}$ M, and $[\text{EDTA}] = 5.0 \times 10^{-4}$ M in a mixture of an acetate buffer (pH 4–6, final concentration = 10 mM) or a phosphate buffer (pH 7–8, final concentration = 10 mM) and DMSO (1:1, v/v). $\lambda_{\text{ex}} = 366$ nm.

Detection of Ag^+ by **2** in the presence of EDTA was relatively fast, and a saturated

signaling was observed after less than 1 min (Figure 5). In addition, probe **2** itself was stable under the measurement conditions, and no measurable changes were observed 5 h after sample preparation.

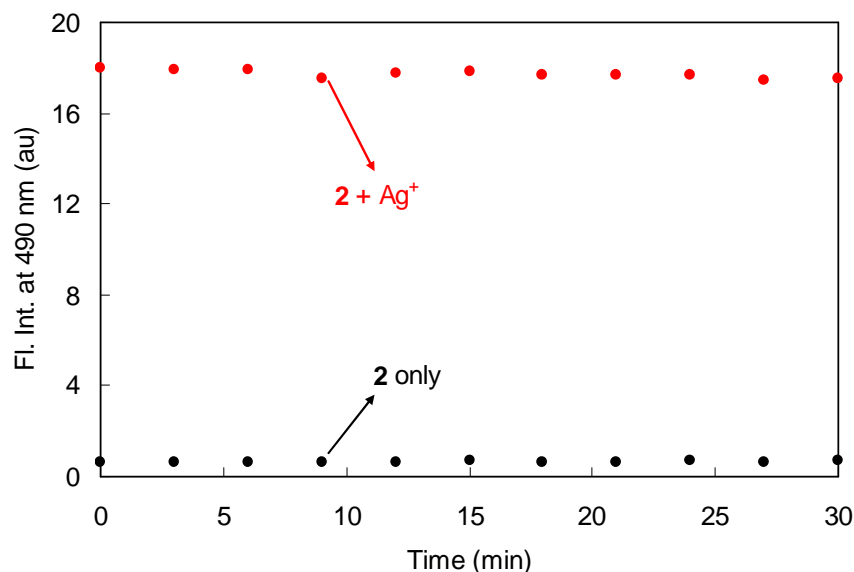


Figure 5. Change in fluorescence intensity of Ag^+ signaling by **2** at 490 nm over time. [**2**] = 5.0×10^{-6} M, $[\text{Ag}^+] = 5.0 \times 10^{-5}$ M. Other conditions are the same as those in Figure 1.

The quantitative signaling properties of **2** were assessed by fluorescence titration with Ag^+ ions. As $[\text{Ag}^+]$ increased, the fluorescence intensity of **2** at 490 nm increased steadily (Figure 6). A plot of the change in fluorescence intensity as a function of $[\text{Ag}^+]$ yielded a useful calibration plot for the determination of Ag^+ ions up to 8.5×10^{-6} M. The minor sigmoidal-type plot observed in the low concentration region ($[\text{Ag}^+] < 1 \mu\text{M}$) could be due to the involvement of Ag^+ ions in additional complex formation equilibria with the chelating agent EDTA. The detection limit for Ag^+ ions was found to be $0.075 \mu\text{M}$, as estimated using the IUPAC recommended procedure ($3s_{b1}/m$), where s_{b1} and m

denote the standard deviation of the blank and the slope of the calibration plot, respectively [46].

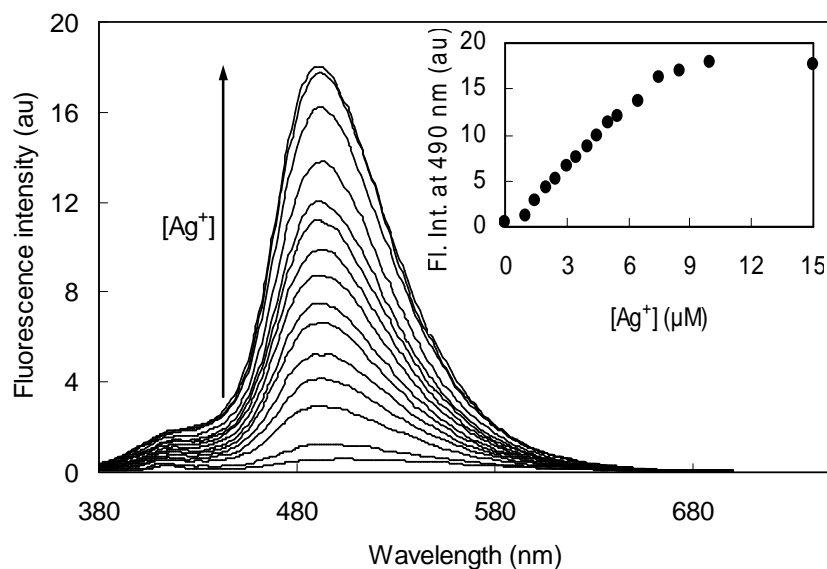


Figure 6. Changes in the fluorescence spectrum of **2** as a function of $[Ag^+]$. Inset: changes in fluorescence intensity at 490 nm. $[2] = 5.0 \times 10^{-6}$ M, $[Ag^+] = 0-1.5 \times 10^{-5}$ M. Other conditions are the same as those in Figure 1.

Finally, a practical application of the probe to the detection of Ag^+ in simulated wastewater samples was demonstrated. Solutions containing varying amounts of Ag^+ ions in simulated wastewater were prepared, and the fluorescence intensities of **2** in these solutions were measured at 490 nm. Simulated wastewater was prepared following literature examples [43,44], and the composition is shown in Table S1, Supplementary data. The obtained calibration plots showed there was a linear relationship between fluorescence intensity and $[Ag^+]$ that held up to 5 μM in simulated wastewater samples

(Figure 7). In parallel to this, images of the signaling solutions were captured using a smartphone (Samsung, Galaxy S7). The change in color was analyzed using a smartphone-embedded app (RGB Grabber). The plot between the green channel level and $[\text{Ag}^+]$ revealed a useful correlation (Figure 8). From the concentration-dependent change in green channel level, a detection limit of $0.76 \mu\text{M}$ was estimated for Ag^+ determination in wastewater samples using a smartphone as a stand-alone signal capturing and processing device.

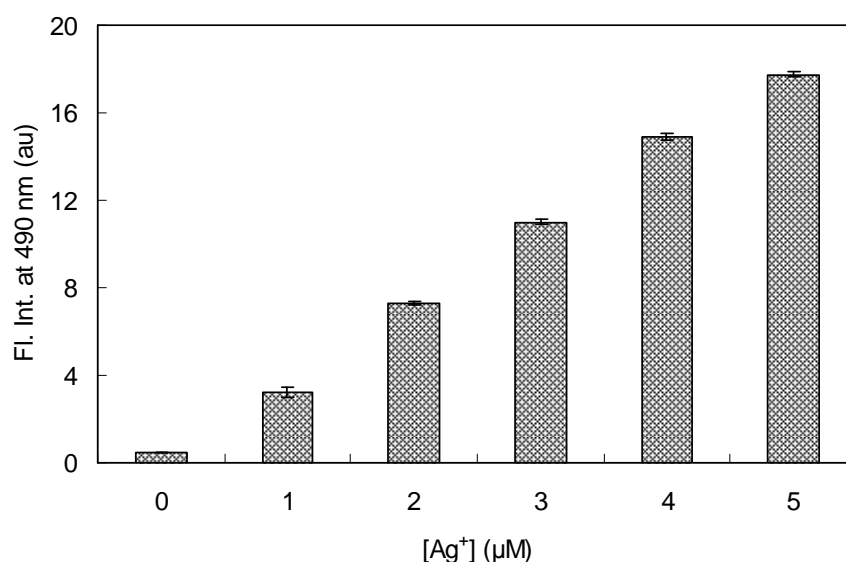


Figure 7. Fluorescence signaling of Ag^+ by **2** in simulated wastewater. $[\mathbf{2}] = 5.0 \times 10^{-6}$ M, $[\text{Ag}^+] = 0\text{--}5.0 \times 10^{-6}$ M. Other conditions are the same as those in Figure 1.

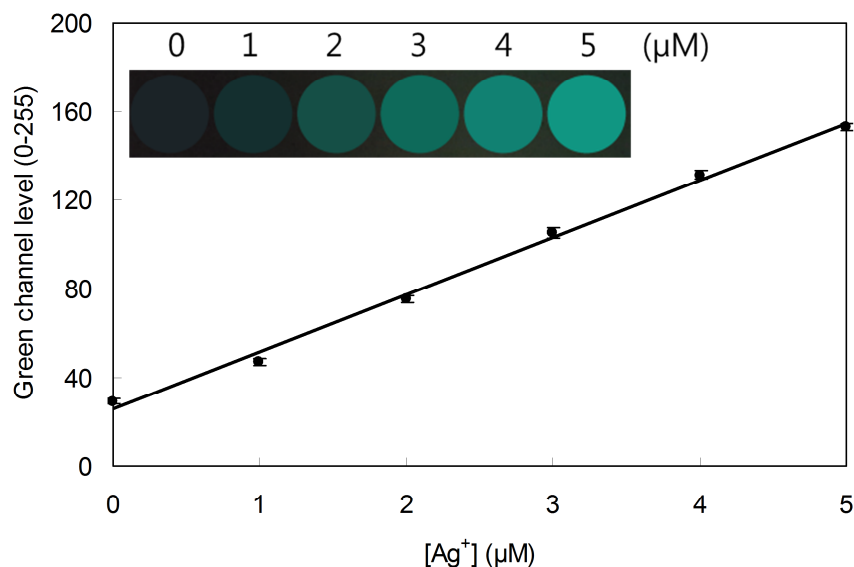


Figure 8. Changes in green channel level as a function of $[\text{Ag}^+]$ in simulated wastewater containing **2** obtained using a smartphone. Inset: fluorescence images under illumination with a UV lamp (365 nm), which were analyzed using an app (RGB Grabber). $[\mathbf{2}] = 5.0 \times 10^{-6}$ M, $[\text{Ag}^+] = 0\text{--}5.0 \times 10^{-6}$ M, and $[\text{EDTA}] = 5.0 \times 10^{-4}$ M in a mixture of an acetate buffered solution (pH 4.0, final concentration = 10 mM) and DMSO (1:1, v/v).

4. Conclusions

We have developed a novel Ag^+ -selective reaction-based probe utilizing the Ag^+ -assisted acetylthiourea-acetylurea transformation of 2-(2-hydroxyphenyl)benzothiazole-based dye. The acetylthiourea moiety satisfactorily functioned as a selective Ag^+ -triggered switching-on handle for the recovery of 2-(2-hydroxyphenyl)benzothiazole fluorescence. The designed probe showed pronounced off-on type fluorescence signaling behavior in the presence of Ag^+ ions.

Interference from Hg^{2+} ions was readily eliminated using a chelating agent, EDTA, as an auxiliary masking agent. The practical application of the system to the detection of Ag^+ in simulated wastewater was successfully demonstrated using a smartphone as a stand-alone data capturing and processing device suitable for field applications.

Acknowledgements

This study was supported by Chung-Ang University Research Scholarship Grants in 2017 (G.Y.P.) and a fund from the National Research Foundation of Korea (NRF) funded by the Korean Government (NRF-2015R1D1A1A01061470).

Appendix. Supplementary data

Supplementary data associated with this article can be found in the online version at doi:*.****.

References

- [1] Wang HH, Xue L, Qian YY, Jiang H. Novel ratiometric fluorescent sensor for silver ions. *Org Lett* 2009;12:292–5.
- [2] Barriada JL, Tappin AD, Evans EH, Achterberg EP. Dissolved silver measurements in seawater. *Trac-Trends Anal Chem* 2007;26:809–17.

- [3] Zhang XB, Han ZX, Fang ZH, Shen GL, Yu RQ. 5,10,15-Tris (pentafluorophenyl) corrole as highly selective neutral carrier for a silver ion-sensitive electrode. *Anal Chim Acta* 2006;562:210–5.
- [4] Ratte HT. Bioaccumulation and toxicity of silver compounds: a review. *Environ Toxicol Chem* 1999;18:89–108.
- [5] Richards RME, Taylor RB, Xing DK. An evaluation of the antibacterial activities of combinations of sulfonamides, trimethoprim, dibromopropamide, and silver nitrate compared with their uptakes by selected bacteria. *J Pharm Sci* 1991;80:861–7.
- [6] Rauser WE. Phytochelatins. *Annu Rev Biochem* 1990;59:61–86.
- [7] Fürst P, Hamer D. Cooperative activation of a eukaryotic transcription factor: interaction between Cu(I) and yeast ACE1 protein. *Proc Natl Acad Sci USA* 1989;86:5267–71.
- [8] Ralston DM, O'Halloran TV. Ultrasensitivity and heavy-metal selectivity of the allosterically modulated MerR transcription complex. *Proc Natl Acad Sci USA* 1990;87:3846–50.
- [9] Asharani P, Wu YL, Gong Z, Valiyaveetil S. Toxicity of silver nanoparticles in zebrafish models. *Nanotechnology* 2008;19:255102–9.
- [10] Lee KJ, Nallathamby PD, Browning LM, Osgood CJ, Xu XHN. In vivo imaging of transport and biocompatibility of single silver nanoparticles in early development of zebrafish embryos. *ACS Nano*. 2007;1:133–43.
- [11] Fabrega J, Fawcett SR, Renshaw JC, Lead JR. Silver nanoparticle impact on bacterial growth: effect of pH, concentration, and organic matter. *Environ Sci Technol* 2009;43:7285–90.

- [12] Kilinc E, Lepane V, Viitak A, Gumgum B. Off-line determination of trace silver in water samples and standard reference materials by cloud point extraction-atomic absorption spectrometry. *Proc Estonian Acad Sci* 2009;58:190–6.
- [13] Wang F, Nandhakumar R, Moon JH, Kim KM, Lee JY, Yoon J. Ratiometric fluorescent chemosensor for silver ion at physiological pH. *Inorg Chem* 2011;50:2240–5.
- [14] Amini MK, Ghaedi M, Rafi A, Mohamadpoor-Baltork I, Niknam K. Silver selective electrodes based on methyl-2-pyridyl ketone oxime, phenyl-2-pyridyl ketone oxime and bis[2-(*o*-carboxythiophenoxy)methyl]-4-bromo-1-methoxybenzene carriers. *Sens Actuators B Chem* 2003;96:669–76.
- [15] Bian L, Ji X, Hu W. A novel single-labeled fluorescent oligonucleotide probe for silver (I) ion detection in water, drugs, and food. *J Agric Food Chem* 2014;62:4870–7.
- [16] Singha S, Kim D, Seo H, Cho SW, Ahn KH. Fluorescence sensing systems for gold and silver species. *Chem Soc Rev* 2015;44:4367–99.
- [17] Karunasagar D, Arunachalam J, Gangadharan S. Development of a ‘collect and punch’ cold vapour inductively coupled plasma mass spectrometric method for the direct determination of mercury at nanograms per litre levels. *J Anal At Spectrom* 1998;13:679–82.
- [18] Li Y, Chen C, Li B, Sun J, Wang J, Gao Y, et al. Elimination efficiency of different reagents for the memory effect of mercury using ICP-MS. *J Anal At Spectrom* 2006;21:94–6.
- [19] Kagan D, Calvo-Marzal P, Balasubramanian S, Sattayasamitsathit S, Manesh KM, Flechsig GU, et al. Chemical sensing based on catalytic nanomotors: Motion-based detection of trace silver. *J Am Chem Soc* 2009;131:12082–3.

- [20] Baron MG, Herrin RT, Armstrong DE. The measurement of silver in road salt by electrothermal atomic absorption spectrometry. *Analyst* 2000;125:123–6.
- [21] Yang L, Sturgeon RE. On-line determination of silver in sea-water and marine sediment by inductively coupled plasma mass spectrometry. *J Anal At Spectrom* 2002;17:88–93.
- [22] Mohadesi A, Taher MA. Stripping voltammetric determination of silver(I) at carbon paste electrode modified with 3-amino-2-mercaptoquinazolin-4(3H)-one. *Talanta* 2007;71:615–9.
- [23] Ceresa A, Radu A, Peper S, Bakker E, Pretsch E. Rational design of potentiometric trace level ion sensors. A Ag⁺-selective electrode with a 100 ppt detection limit. *Anal Chem* 2002;74:4027–36.
- [24] Li X, Gao X, Shi W, Ma H. Design strategies for water-soluble small molecular chromogenic and fluorogenic probes. *Chem Rev* 2013;114:590–659.
- [25] Carter KP, Young AM, Palmer AE. Fluorescent sensors for measuring metal ions in living systems. *Chem Rev* 2014;114:4564–601.
- [26] Yang Y, Zhao Q, Feng W, Li F. Luminescent chemodosimeters for bioimaging. *Chem Rev* 2013;113:192–270.
- [27] Tang Y, Lee D, Wang J, Li G, Yu J, Lin W, et al. Development of fluorescent probes based on protection–deprotection of the key functional groups for biological imaging. *Chem Soc Rev* 2015;44:5003–15.
- [28] Kaur K, Saini R, Kumar A, Luxami V, Kaur N, Singh P, et al. Chemodosimeters: an approach for detection and estimation of biologically and medically relevant metal ions, anions and thiols. *Coord Chem Rev* 2012;256:1992–2028.

- [29] Chase M, Czarnik AW. Fluorimetric chemodosimetry. Mercury(II) and silver(I) indication in water via enhanced fluorescence signaling. *J Am Chem Soc* 1992;114:9704–5.
- [30] Zhang X, Xu Y, Guo P, Qian X. A dual channel chemodosimeter for Hg^{2+} and Ag^+ using a 1,3-dithiane modified BODIPY. *New J Chem* 2012;36:1621–5.
- [31] Tsukamoto K, Shinohara Y, Iwasaki S, Maeda H. A coumarin-based fluorescent probe for Hg^{2+} and Ag^+ with an *N*'-acetylthioureido group as a fluorescence switch. *Chem Commun* 2011;47:5073–5.
- [32] Shi W, Sun S, Li X, Ma H. Imaging different interactions of mercury and silver with live cells by a designed fluorescence probe rhodamine B selenolactone. *Inorg Chem* 2009;49:1206–10.
- [33] Chatterjee A, Santra M, Won N, Kim S, Kim JK, Kim SB, et al. Selective fluorogenic and chromogenic probe for detection of silver ions and silver nanoparticles in aqueous media. *J Am Chem Soc* 2009;131:2040–1.
- [34] Liang J, Ai X, He Z, Pang D. Functionalized CdSe quantum dots as selective silver ion chemodosimeter. *Analyst* 2004;129:619–22.
- [35] Hien NK, Bao NC, Nhung NTA, Trung NT, Nam PC, Duong T, et al. A highly sensitive fluorescent chemosensor for simultaneous determination of Ag(I), Hg(II), and Cu(II) ions: design, synthesis, characterization and application. *Dyes Pigment* 2015;116:89–96.
- [36] Kwon JE, Park SY. Advanced organic optoelectronic materials: Harnessing excited-state intramolecular proton transfer (ESIPT) process. *Adv Mater* 2011;23:3615–42.

- [37] Cui L, Zhu W, Xu Y, Qian X. A novel ratiometric sensor for the fast detection of palladium species with large red-shift and high resolution both in aqueous solution and solid state. *Anal Chim Acta* 2013;786:139-45.
- [38] Santra M, Roy B, Ahn KH. A “reactive” ratiometric fluorescent probe for mercury species. *Org Lett* 2011;13:3422-5.
- [39] Hu R, Feng J, Hu D, Wang S, Li S, Li Y, et al. A rapid aqueous fluoride ion sensor with dual output modes. *Angew Chem Int Ed* 2010;49:4915-8.
- [40] Chen JS, Zhou PW, Zhao L, Chu TS. A DFT/TDDFT study of the excited state intramolecular proton transfer based sensing mechanism for the aqueous fluoride chemosensor BTTPB. *RSC Adv* 2014;4:254-9.
- [41] Li G, Zhu D, Liu Q, Xue L, Jiang H. Rapid detection of hydrogen peroxide based on aggregation induced ratiometric fluorescence change. *Org Lett* 2013;15:924-7.
- [42] Choi MG, Lee SH, Jung YU, Hong JM, Chang SK. Fluorescence signaling of BF_3 species by transformation of an ESIPT dye to its difluoroboron adduct. *Sens Actuators B Chem* 2017;251:713-9.
- [43] Tchobanoglous G, Burton FL. *Wastewater engineering: treatment disposal reuse*. New York: McGraw-Hill; 1991. p. 1820.
- [44] Wong YC, Moganaragi V, Atiqah NA. *Physico-chemical investigations of semiconductor industrial wastewater*. *Orient J Chem* 2013;29:1424-8.
- [45] Harris DC. *Quantitative chemical analysis*. 8th ed. New York: Freeman; 2010. p. 241-3.
- [46] Harris DC. *Quantitative chemical analysis*. 8th ed. New York: Freeman; 2010. p. 103-5.

Figure Captions

Scheme 1. Preparation of Ag⁺-selective acetylthiourea (**2**) and thioamide (**4**) probes.

Scheme 2. Ag⁺ signaling by desulfurization of **2**.

Figure 1. Ag⁺-selective signaling of **2** in the presence of a masking agent (EDTA). Inset: changes in fluorescence spectrum. [**2**] = 5.0 × 10⁻⁶ M, [Mⁿ⁺] = 5.0 × 10⁻⁵ M, and [EDTA] = 5.0 × 10⁻⁴ M in a mixture of an acetate buffer (pH 4.0, final concentration = 10 mM) and DMSO (1:1, v/v). λ_{ex} = 366 nm.

Figure 2. Partial ¹H NMR spectra of **2** and **2** in the presence of Ag⁺ (**2** + Ag⁺). [**2**] = 5.0 × 10⁻³ M, [AgClO₄] = 1.0 × 10⁻² M in DMSO-d₆. The spectrum of (**2** + Ag⁺) was obtained after purification of the signaling product by passing it through a silica plug.

Figure 3. Changes in fluorescence spectrum of **2** when detecting Ag⁺ in the presence of various metal ions as background (upper). Fluorescence intensity ratio ($I_{(\text{Metal ion}+\text{Ag(I)})}/I_{\text{Ag(I)}}$) of **2** at 490 nm (lower). [Ag⁺] = [Mⁿ⁺] = 5.0 × 10⁻⁵ M. Other conditions are the same as those in Figure 1.

Figure 4. Effect of pH on the selective fluorescence signaling of Ag⁺ by **2** expressed by $I_{\text{Ag(I)}}/I_{\text{Hg(II)}}$. [**2**] = 5.0 × 10⁻⁶ M, [Ag⁺] = [Hg²⁺] = 5.0 × 10⁻⁵ M, and [EDTA] = 5.0 × 10⁻⁴ M in a mixture of an acetate buffer (pH 4–6, final concentration = 10 mM) or a phosphate buffer (pH 7–8, final concentration = 10 mM) and DMSO (1:1, v/v). λ_{ex} = 366 nm.

Figure 5. Change in fluorescence intensity of Ag^+ signaling by **2** at 490 nm over time. $[\text{Ag}^+] = 5.0 \times 10^{-5}$ M. Other conditions are the same as those in Figure 1.

Figure 6. Changes in the fluorescence spectrum of **2** as a function of $[\text{Ag}^+]$. Inset: changes in fluorescence intensity at 490 nm. $[\text{Ag}^+] = 0-1.5 \times 10^{-5}$ M. Other conditions are the same as those in Figure 1.

Figure 7. Fluorescence signaling of Ag^+ by **2** in distilled water and simulated wastewater. $[\text{Ag}^+] = 0-5.0 \times 10^{-6}$ M. Other conditions are the same as those in Figure 1.

Figure 8. Changes in green channel level as a function of $[\text{Ag}^+]$ in simulated wastewater containing **2** obtained using a smartphone. Inset: fluorescence images under illumination with a UV lamp (365 nm), which were analyzed using an app (RGB Grabber). $[\mathbf{2}] = 5.0 \times 10^{-6}$ M, $[\text{Ag}^+] = 0-5.0 \times 10^{-6}$ M, and $[\text{EDTA}] = 5.0 \times 10^{-4}$ M in a mixture of an acetate buffered solution (pH 4.0, final concentration = 10 mM) and DMSO (1:1, v/v).

Highlights:

- A new reaction-based Ag^+ -selective fluorescence signaling probe has been explored.
- Signaling was based on Ag^+ -induced desulfurization of acetylthiourea to acetylurea.
- Interference from Hg^{2+} was effectively suppressed using EDTA as a masking agent.
- The probe could easily determine Ag^+ level in simulated wastewater using a smartphone.